NCC 2020 Tutorial

Energy Harvesting and RF Energy Transfer aided Sustainable IoT Networks

Swades De

Department of Electrical Engineering
Communication Networks Research Group
Indian Institute of Technology Delhi

[ACKNOWLEDGMENT: Priyadarshi Mukherjee, Sharda Tripathi, Vini Gupta, Deepak Mishra, K Kaushik, Suraj Suman]

February 21, 2020

Presentation Outline

My Current Research Directions

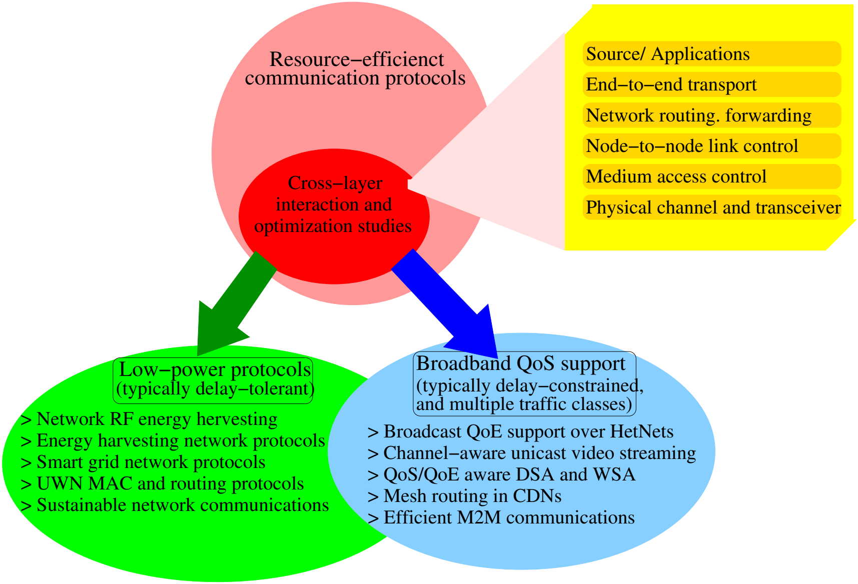

Background and Motivation

- Explosive growth in high throughput applications. Global Internet traffic estimated to increase more than five times between 2018 and 2024[1]

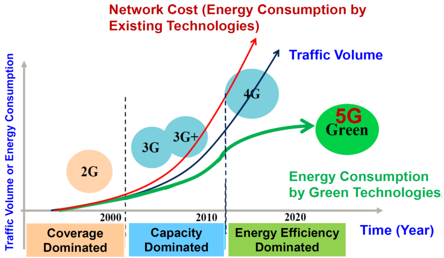

- This leads to proportionate increase in energy consumption of wireless networks
- Hence "energy-efficient green communication" is gaining popularity in industry as well as academics[2]

[1] "The power of 5G," *Ericsson Mobility Report,* Nov., 2018.

[2] Available: http://www.chaire-ueb.cominlabs.ueb.eu/ .

Background and Motivation (contd.)

- IoT devices are expected to increase at a compound annual growth rate of 7% by 2022[3] ⇒ energy sustainability is of keen interest

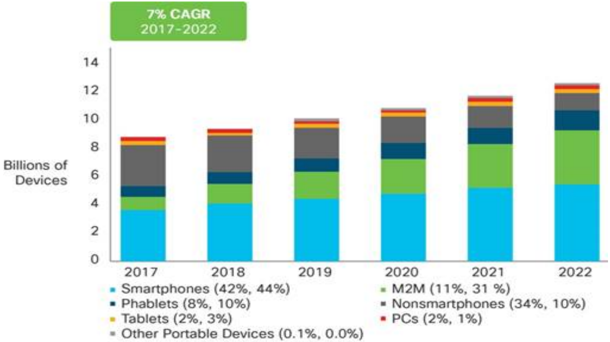

- Limited battery capacity of IoT devices is a major bottleneck
- Mechanisms to ensure the perpetual operation of growing number of devices is of very high importance

[3] Cisco, *Cisco Visual Networking Index: Global Mobile Data Traffic Forecast Update, 2016-2021*. Cisco White Paper, 2017.

Network Performance Measures

- Problems encountered in computer communication networks
  - Congestion/delay
  - Blocked calls and dropped calls
  - Poor QoS/QoE
  - Concerns of resource efficiency
- These affect customer satisfaction and market revenue
- Need for **network planning**: e.g., routing, switching, multiplexing
- Need for **resource management**: e.g., frequency reuse, energy usage
- Performance evaluation: **Modeling and analysis**
  - Freedom of adjusting parameters during network planning and execution
  - Helps in finding the performance bottlenecks

Performance Evaluation Techniques

Three main evaluation techniques

- **Measurement**
- System **simulation**
- Mathematical or **analytical** modeling

Comparison of three techniques

Technique	Requirements	Merits	Demerits
Measurement	Instrumentation and experimental hardware	Most accurate	1. Expensive and time consuming 2. Non-repetitive measurements 3. Not compatible with future designs
Simulation	1. Simulator 2. Programming skills	1. High control over parameters and workload 2. Compatible with future system designs with some extra effort	1. Less accuracy 2. Large effort
Analysis	1. Systems level understanding 2. Mathematical skills	1. Least effort 2. High control over parameters and workload 3. Smooth compatibility to future system designs	1. Least accurate 2. Unrealistic assumptions

Stochastic Process

Definition: A stochastic process S is a family of random variables $X(t)$, each defined on some sample space Ω and function of time t defined on parameter space T.

- In simple terms, *a set of random variables which are function of time*
- T, normally considered as *time* can be either discrete or continuous: **Discrete or continuous time process**
  - every month: discrete
  - real time: continuous
- Ω denoting *set of values $X(t)$ can take,* can be discrete or continuous: **Discrete or continuous state process**
  - number of active tasks: discrete
  - time delay in communication network: continuous

Classification

Relationship among some interesting stochastic processes[4]

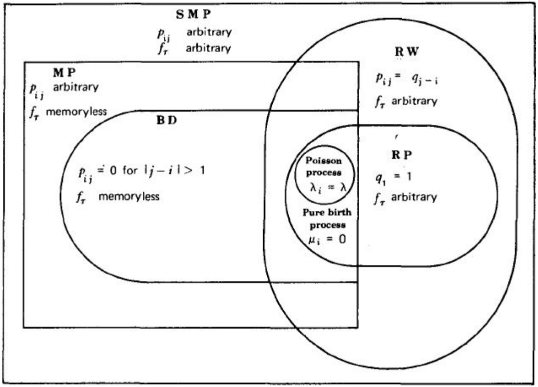

SMP: Semi-Markov Process;
MP: Markov Process;
BD: Birth-Death Process;
RW: Random Walk;
RP: Random Process

i,j: States;
$\mathbf{p_{ij}}$: Transition probability from state i to j;
$\mathbf{f_\tau}$: Distribution of time between transitions;
q: Random Walk;
λ: Birth/arrival rate
μ: Death/service rate

[4] L. Kleinrock, *Queueing Systems, volume I: Theory*. Wiley Interscience, 1975.

Limitation of Classical Stochastic Analysis

Shortcomings of Stochastic Analysis:

- Stationarity of the process is assumed, which may not be true to real world applications
- Mathematical model thus obtained is only an approximate representation of the process

Data-driven Optimization Studies:

- Adaptive to the dynamics of real world systems
- Robust, but can be computationally intensive

Motivations to Cross-Layer Protocol Optimization Studies

- Basic network layer concepts

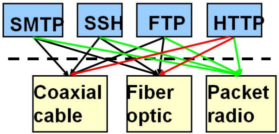

$O(ma)$ overhead
to add a apps and m media

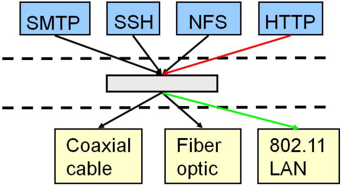

$O(1)$ overhead to add app/media

Network layering motivation

  - Pros and cons of layer-based approach
- **Miniaturization** and **personalization** of mobile wireless devices
- **Green communication systems**
  - Need for **network planning**: e.g., routing, switching, multiplexing
  - Need for **resource management**: e.g., frequency reuse, energy usage
- Cross-layered study objectives and concepts
  - Pros and cons of cross-layered approach
- Need for **system-level performance modeling and analysis**

Cross-Layer Interactions and Examples

- Functionalities of a protocol layer are influenced by the other layers
- Accounting such dependencies make the protocol design more responsive to the system's needs as a whole

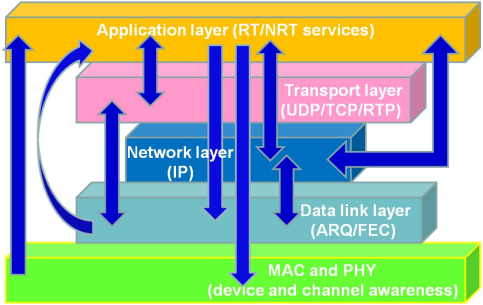

Cross-layering examples

- Physical layer aware media access control, e.g., in UWSN
- Physical layer aware link layer error control, e.g., stop-and-wait protocol
- Physical channel and device limitations aware source coding adaptation
- Energy efficiency and energy harvesting toward green communications

Link-level Objectives and Current Practices

- Node-level error and flow control
  - Error-prone wireless channel: use error control schemes (AMC, ARQ, FEC)
  - Time-varying channel: ARQ vs. FEC (error bursts, return channel, delay)
  - Limited energy of of portable devices: energy efficiency of interest
- Classical ARQ schemes: SW, GBN, SR
- PHY solutions: MCS (e.g., n-QAM, Hamming codes, RS codes)
- Hybrid ARQ: FEC+limited ARQ
- "Channel-aware" link-layer transmission solutions
  - Probing-based [Zorzi and Rao (IEEE Trans. Comp. '97)]
  - Probabilistic automata [Sampath et al. (Intl. J. WCMC, 2007)]
- Window flow control (Transport layer)

- Seek and utilize the channel information to adapt *suitably*
  - Need to appropriately filter out the required channel information

Markov Modeling of Wireless Channel

- Packet error follow a **first-order Markov model** with transition matrix:[5]

$$M(i) = \begin{bmatrix} p_{11}(i) & p_{12}(i) \\ p_{21}(i) & p_{22}(i) \end{bmatrix} \quad \text{and} \quad M(1) = \begin{bmatrix} p_{11} & p_{12} \\ p_{21} & p_{22} \end{bmatrix}$$

  $p_{11} = 1 - p_{12}$ $(p_{21} = 1 - p_{22})$ probability of successful (unsuccessful) transmissions
- Marginal probability of packet error $\varepsilon = 1 - \frac{p_{21}}{1-p_{11}+p_{21}}$
- Average probability of block error $\varepsilon = P[1] = E[P_w(v)] = \int_0^\infty P_w(a) f_v(a) da$

  where $f_v(a)$ is pdf of **fading envelope**
- Probability that two successive blocks are in error is:

$$P[1,1] = E[P_w(v_1)P_w(v_2)] = \int_0^\infty \int_0^\infty P_w(a_1)P_w(a_2) f_{v_1 v_2}(a_1, a_2) da_1 da_2$$

$$\text{and} \quad p_{21} = 1 - P[1|1] = 1 - \frac{P[1,1]}{P[1]} = 1 - \frac{P[1,1]}{\varepsilon}$$

- For **2nd order SC diversity**, conditional probability of unsuccessful reception:

$$P_w(x) = 1 - P[A(x)] \quad \text{with} \quad x = \max\left\{v^{(1)}, v^{(2)}\right\}$$

$$\text{where} \quad F_v(a) = P\left[v^{(1)} \le a\right] = P\left[v^{(2)} \le a\right]$$

---

[5] M. Zorzi, R. R. Rao, and L. B. Milstein, "ARQ error control for fading mobile radio channels", *IEEE Trans. Veh. Technol.*, vol. 46, no. 2, pp. 445–455, 1997.

Markov Modeling of Wireless Channel – II

- $F_x(a) = [F_v(a)]^2$ and $\varepsilon = E[P_w(x)] = \int_0^\infty P_w(a)2F_v(a)f_v(a)da$
- $F_{x_1x_2}(a_1, a_2) = [F_{v_1v_2}(a_1, a_2)]^2$ and

$$P_{(d)}[1,1] = E[P_w(x_1)P_w(x_2)] = \int_0^\infty \int_0^\infty P_w(a_1)P_w(a_2)f_{x_1x_2}(a_1, a_2)\, da_1 da_2$$

- If $P_w(v) = \begin{cases} 0, & v^2 > P_0 \\ 1, & v^2 \leq P_0, \end{cases}$, then

$$\varepsilon = F_v(\sqrt{P_0}),\ P[1,1] = F_{v_1v_2}\left(\sqrt{P_0}, \sqrt{P_0}\right) \text{ and } \varepsilon_{(d)} = \varepsilon^2$$

$$P_{(d)}[1,1] = F_{v_1v_2}\left(\sqrt{P_0}, \sqrt{P_0}\right) \text{ and } \varepsilon_{(d)} = \varepsilon^2$$

$$P_{(d)}[1,1] = \left[F_{v_1v_2}\left(\sqrt{P_0}, \sqrt{P_0}\right)\right]^2,\ \varepsilon_{(d)} = \left(P_{(d)}[1,1]\right)^2,\ p_{21(d)} = 1-(1-p_{21})^2$$

- For Rayleigh fading, the pdf of envelope is: $f_v(a) = 2ae^{-a^2}$
- Joint pdf is $f_{v_1v_2}(a_1, a_2) = \frac{a_1a_2}{1-\rho^2}e^{-\frac{a\left(a_1^2+a_2^2\right)}{2(1-\rho^2)}} I_0\left(\frac{\rho a_1 a_2}{1-\rho^2}\right)$ with $\rho = J_0(2\pi f_D T)$
- $\varepsilon = 1 - e^{-P_0}$, $p_{21} = \frac{Q(\theta, p\theta), Q(p\theta, \theta)}{e^{P_0}-1}$, where $\theta = \sqrt{\frac{2P_0}{1-\rho^2}}$.

Stop-and-Wait ARQ Protocols[6]

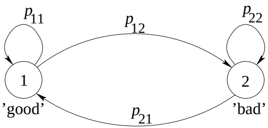

- Performance measures:
  - *Data throughput* $\mathcal{R}$: Successful frames/s:
    $\mathcal{R} \triangleq \lim_{t\to\infty} \frac{E\{\text{number of data frames successful in time } t\}}{t}$
  - *Energy efficiency* $\mathcal{E}$: Energy consumption per successful data frame, including tx and rx energy per data frame e_d and per ACK/NAK frame e_a, per slot idling energy e_w and total energy e_p per probing frame.

- $p_{11}(m) = \frac{[p_{21}+(1-p_{21}-p_{12})^m p_{12}]}{p_{21}+p_{12}}, \quad p_{21}(m) = \frac{p_{21}[1-(1-p_{21}-p_{12})^m]}{p_{21}+p_{12}}$

SW cycle

Duration from an unsuccessful frame to the end of its successful transmission.

- $E\{\mathbf{K}\} = \sum_{\kappa=1}^{\infty} \kappa \cdot \Pr[\mathbf{K} = \kappa] = \frac{p_{12}(m)+p_{21}(m)}{p_{21}(m)}$
- Throughput of basic SW: $\mathcal{R}_{SW} = \frac{1}{E\{\mathbf{K}\}\cdot m\cdot s}$
- Energy consumed per successful data frame in basic SW:
  $\mathcal{E}_{SW} = E\{\mathbf{K}\}\left[e_d + e_a + (m-1)e_w\right]$

[6] S. De, A. Sharma, R. Jantti, and D. H. Cavdar, "Channel adaptive stop-and-wait automatic repeat request protocols for short-range wireless links", *IET Commun.*, vol. 6, no. 14, pp. 2124–2137, 2012.

Channel Oblivious Probing (COP) Scheme based SW

- Once a NAK is received, transmitter enters probing mode, with a periodicity independent of fading margin
- Probing frames are continued until a probing ACK is received
- Average number $E\{\mathbf{P}\}$ in a set of contiguous probing is: $E\{\mathbf{P}\} = \frac{1}{p_{21}(t_p)}$

COP cycle

Length of a cycle in COP based SW is defined as the duration between two probing phases, which gives a single probing ACK.

- $E\{\mathbf{K}\} = \frac{1+p_{12}(m)}{p_{12}(m)}$
- Data throughput in COP based SW: $\mathcal{R}_{COP} = \frac{E\{\mathbf{K}\}-1}{(E\{\mathbf{K}\}-1)ms+s+T_p+E\{\mathbf{P}\}t_p s+2T_p}$
- Average energy consumed per successful data frame is approximately: $\mathcal{E}_{COP} = \frac{E\{\mathbf{K}\}(e_d+e_a)+(E\{\mathbf{K}\}-1)(m-1)e_w+E\{\mathbf{P}\}(e_p+t_p e_w)}{E\{\mathbf{K}\}-1}$

Channel Aware Probing and Channel Aware SW

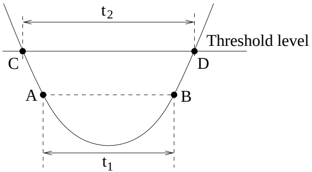

- Average waiting in CAP3: $E\{\mathbf{w_p}\} = E\{\mathbf{W}^{(1)}\} + E\{\mathbf{W}^{(2)}\}\frac{p_{22}(w_1)}{p_{21}(w_2)}$
- $E\{\mathbf{W}^{(x)}\} = \sum_{i=0}^{L-1} W_i^{(x)}\, p_{i|nak}\ x = 1, 2;\ \ E\{\mathbf{P}\} = \frac{p_{21}(w_2)+p_{22}(w_1)}{p_{21}(w_2)}$
- $\mathcal{R}_{CAP3} = \frac{E\{\mathbf{K}\}-1}{\left[\left(E\{\mathbf{K}\}-1\right)ms+s+T_p\right]+\left\lceil\frac{E\{\mathbf{w_p}\}}{s}\right\rceil s+2T_p}$
- $\mathcal{E}_{CAP3} = \frac{E\{\mathbf{K}\}(e_d+e_a)+\left(E\{\mathbf{K}\}-1\right)(m-1)e_w+E\{\mathbf{P}\}e_p+\left\lceil\frac{E\{\mathbf{w_p}\}}{s}\right\rceil e_w}{E\{\mathbf{K}\}-1}$

CASW cycle

A *CASW cycle* is the duration between the ends of two consecutive lost data frames.

- $\mathcal{R}_{CASW} = \frac{E\{\mathbf{J}\}}{(E\{\mathbf{J}\}ms+s+T_p)+\pi s};\ \ E\{\mathbf{J}\} = \frac{p_{21}(\pi)}{p_{12}(m)}$
- $\mathcal{E}_{CASW} = \frac{1}{E\{\mathbf{J}\}}\left[(E\{\mathbf{J}\}+1)(e_d+e_a)+E\{\mathbf{J}\}(m-1)e_w+\pi e_w\right]$

Effect of Mobility and Energy Saving-Throughput Tradeoff

- Effect of mobility on Throughput and Energy consumption performance

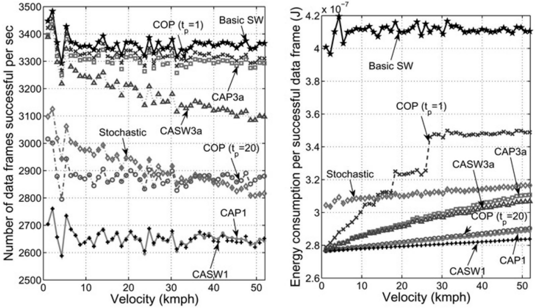

- Performance improvement provided by proposed schemes over basic SW protocol

Energy saving (E-gain) and throughput trade-off (R-loss) in CASW1 and CAP3a protocols over basic SW protocol at different fading margins (FM), $f_D = 50$ Hz

FM, dB	CASW1		CAP3a	
	E-gain, %	R-loss, %	E-gain, %	R-loss, %
4	29.9	21.5	29.4	2.3
6	19.9	13.0	19.4	1.4
8	13.0	8.0	12.3	1.0
10	8.2	5.2	7.7	0.8
12	5.0	3.4	4.7	0.6

ARQ-based switched antenna diversity in Markov channels[7]

- $T_{R_A} = \begin{pmatrix} p_1 & p_3 \\ p_4 & p_2 \end{pmatrix}$, $T_{R_B} = \begin{pmatrix} q_1 & q_3 \\ q_4 & q_2 \end{pmatrix}$
- $\text{PER}_A = \frac{1-p_1}{2-p_1-p_2}$ and $\text{PER}_B = \frac{1-q_1}{2-q_1-q_2}$
- $P =$

$$\begin{bmatrix} p_1q_1 & p_1q_3 & p_3q_1 & p_3q_3 & 0 & 0 & 0 & 0 \\ p_1q_4 & p_1q_2 & p_3q_4 & p_3q_2 & 0 & 0 & 0 & 0 \\ 0 & 0 & 0 & 0 & p_4q_1 & p_2q_1 & p_4q_3 & p_2q_3 \\ 0 & 0 & 0 & 0 & p_4q_4 & p_2q_4 & p_4q_2 & p_2q_2 \\ 0 & 0 & 0 & 0 & p_1q_1 & p_3q_1 & p_1q_3 & p_3q_3 \\ 0 & 0 & 0 & 0 & p_4q_1 & p_2q_1 & p_4q_3 & p_2q_3 \\ p_1q_4 & p_1q_2 & p_3q_4 & p_3q_2 & 0 & 0 & 0 & 0 \\ p_4q_4 & p_4q_2 & p_2q_4 & p_2q_2 & 0 & 0 & 0 & 0 \end{bmatrix}$$

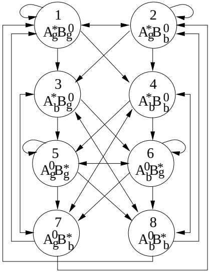

- Throughput of the SSC-ARQ combined scheme:
  $\eta_{SSC-ARQ} = \pi_1 + \pi_2 + \pi_5 + \pi_6$
- For symmetrical channels ($p_1 = q_1,\ p_2 = q_2$),
  $\eta_{SSC-ARQ-sym} = \frac{(1-p_2)^2 + (1-p_1)(1-p_2)(p_1+p_2)}{(2-p_1-p_2)^2}$
- Throughput of ARQ system with only one receive antenna: $\eta_{ARQ} = (1 - \text{PER}) = \frac{1-p_2}{2-p_1-p_2}$
- Throughput gain: $\text{Gain} = \eta_{SSC-ARQ} - \eta_{ARQ}$

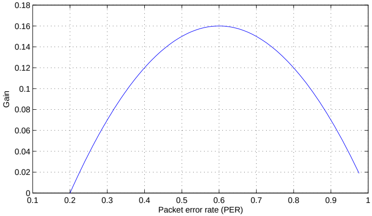

[7] S. Chakraborty, R. Roy, and S. De, "ARQ-based switched antenna diversity in markov channels", *IET Electron. Lett.*, vol. 44, no. 25, pp. 1475–1476, 2008.

Exploiting Short-term Channel State

- Link layer communication between a node pair in mobile environment
- System considered is slotted, slot duration= T_p seconds
- Assumptions:
  - Frames always present at Tx
  - Channel invariant in a frame duration Υ_f; may vary from frame to frame[8]
- Depending on received signal quality, Rx sends ACK/NAK
- In case of NAK, Rx also sends the useful information, such as signal strength information (SSI) and Doppler frequency f_D[9]

[8] Q. Liu, S. Zhou, and G. Giannakis, "Cross-layer combining of adaptive modulation and coding with truncated ARQ over wireless links", *IEEE Trans. Wireless Commun.*, vol. 3, no. 5, pp. 1746–1755, 2004.

[9] C. Tepedelenlioglu, A. Abdi, G. B. Giannakis, and M. Kaveh, "Cross-layer combining of adaptive modulation and coding with truncated ARQ over wireless links", *Wireless Commun. Mobile Comput.*, vol. 1, no. 2, pp. 221–242, 2001.

Time Derivative of Fading Envelope

- For transmission power P at Tx and h being instantaneous channel gain, signal strength indicator (SSI) at Rx is $X = \sqrt{P}|h|$
- Since X is just $|h|$ multiplied by constant $\sqrt{P}$, X provides the same information as h
- We use $\dot{X} \triangleq \frac{dX}{dt}$ in our proposed channel-aware protocols
- $f_{\dot{X}}(\dot{x})$ is always $\mathcal{N}(0, \sigma)$ irrespective of channel fading distribution[10]. Only σ changes depending on fading distribution

Approach using $\dot{X}$ is general, independent of fading distributions

[10] S. Cotton, "Second-Order Statistics of κ-μ Shadowed Fading Channels," *IEEE Trans. Veh. Technol.*, vol. 65, no. 10, pp.8715-8720,2016.

Probability of SSI Staying Below A Threshold

- Let SSI from Rx at time t is $X = X_o (< X_{th})$
- From X_o, estimate N_g (number of slots that X will continue to remain below X_{th})
- Probability that X will not reach X_{th} in the next time slot:

$$\begin{aligned} \Pr\{X(t+T_p) < X_{th}\} &= \Pr\left\{X(t) + \dot{X} \cdot T_p < X_{th}\right\} \\ &= \Pr\{X_0 + X_1 < X_{th}\} \qquad (1) \end{aligned}$$

$X_1 = \dot{X} \cdot T_p$ is a RV denoting temporal variation of X in one slot, where $\dot{X}$ is a Gaussian RV

SSI Staying Below A Threshold in Next 1 Slot

- As $X_o + X_1$ is SSI, $X(t+T_p) \in [0, \infty)$, i.e., $X_1 \in [-X_0, \infty)$
- X_1 is a truncated Gaussian RV:

$$f_{X_1}(x_1) = \begin{cases} \frac{1}{\sqrt{2\pi}\sigma_1\left[1-\Phi_1\left(-\frac{X_0}{\sigma_1}\right)\right]} e^{-\frac{x_1^2}{2\sigma_1^2}} & x_1 \geq -X_0 \\ 0 & \text{elsewhere} \end{cases} \quad (2)$$

$$\Phi(p) = \int_{-\infty}^{p} \frac{1}{\sqrt{2\pi}} e^{-\frac{t^2}{2}} dt$$

- Hence we obtain (1) as $\Pr\{X_0 + X_1 < X_{th}\} = \int_{-\infty}^{X_{th}-X_0} f_{X_1}(\alpha) d\alpha$

Probability of SSI Staying < A Threshold in Next N_g Slots

- Similarly, probability that X will not reach X_{th} in next N_g slots:

$$\Pr\left\{X_o + X_1 < X_{th}, \ldots, X_o + X_{N_g} < X_{th}\right\} = \int_{-\infty}^{X_{th}-X_o} \cdots \int_{-\infty}^{X_{th}-X_o} f_{\boldsymbol{X}}(\boldsymbol{x}, \boldsymbol{\Sigma}, -\boldsymbol{X_o}) d\boldsymbol{x} \quad (3)$$

$f_{\boldsymbol{X}}(\boldsymbol{x}, \boldsymbol{\Sigma}, -\boldsymbol{X_o})$ is a truncated N_g-variate Gaussian distribution [11]

$$f_{\boldsymbol{X}}(\boldsymbol{x}, \boldsymbol{\Sigma}, -\boldsymbol{X_o}) = \frac{e^{-\frac{1}{2}\boldsymbol{x}^T \boldsymbol{\Sigma}^{-1} \boldsymbol{x}}}{\int_{-\boldsymbol{X_o}}^{\infty} e^{-\frac{1}{2}\boldsymbol{x}^T \boldsymbol{\Sigma}^{-1} \boldsymbol{x}} d\boldsymbol{x}}; \quad \boldsymbol{x} \in \mathbb{R}^{N_g}_{\geq -\boldsymbol{X_o}} \quad (4)$$

$$\boldsymbol{X} = [X_1, \ldots, X_{N_g}]^T, \quad -\boldsymbol{X_o} = -X_o[\overbrace{1, \ldots, 1}^{N_g \text{ times}}]^T, \quad \boldsymbol{\Sigma} = \mathbb{E}[\boldsymbol{X}\boldsymbol{X^T}],$$

$\mathbb{R}^{N_g}_{\geq -\boldsymbol{X_o}} = \left\{\boldsymbol{x} \in \mathbb{R}^{N_g} : \boldsymbol{x} \geq -\boldsymbol{X_o}\right\}$, and $\int_{-\boldsymbol{X_o}}^{\infty}$ is an N_g-dimensional integral

[11] W. C. Horrace, "Some results on the multivariate truncated normal distribution," *Journal of Multivariate Analysis,* vol. 94, no. 1, pp. 209-221, 2005.

Dynamic Stop-and-Wait Protocol (D-SW)[12]

- Tx sends data frames every β slot ($\beta \geq 1$) when $X_0 \geq X_{th}$ and regularly receives ACK for each data frame
- Based on SSI obtained from a NAK when $X_0 < X_{th}$, Tx waits for an interval of $T_{bg}(= N_g^* \cdot T_p)$ slots before next transmission
- N_g^* estimation is based on f_D and SSI received over NAK
- No periodicity associated with estimated N_g^*
- D-SW directly resumes data transmission after waiting for N_g^* slots

f_D always does not imply a mobile scenario. It also portrays scenarios with static Tx-Rx but mobile scatterers in between them.

[12] P. Mukherjee, D. Mishra, and S. De "Exploiting Temporal Correlation in Wireless Channel for Energy-Efficient Communication," *IEEE TGCN*, Dec. 2017.

Optimal N_g Estimation

- For given acceptable error ϵ, maximum possible value of N_g is estimated
- (P1) is solved to obtain N_g for given set of system parameters (f_D and T_p), X_o, X_{th}, and ϵ:

$$\text{(P1)} \quad : \underset{N_g \geq 0}{\text{maximize}} \; N_g \tag{5}$$

$$\text{subject to} \quad \Pr\left\{X_o + X_1 < X_{th}, \ldots, X_o + X_{N_g} < X_{th}\right\} \geq 1 - \epsilon$$

- $\Pr\left\{X_o + X_1 < X_{th}, \ldots, X_o + X_{N_g} < X_{th}\right\}$ is calculated using (3)
- X_i like X_1 is also a zero mean truncated Gaussian RV with variance $\sigma_i^2 = i\sigma_1^2$
- To solve (5), we define lower bound N_g^{lb} and upper bound N_g^{ub} for a given set of system parameters

N_g^{lb} Calculation

- Assuming complete independence among all X_i, we get

$$\Pr\{X_o + X_1 < X_{th}, \ldots, X_o + X_N < X_{th}\} = \prod_{i=1}^{N} \Pr\{X_o + X_i < X_{th}\} \tag{6}$$

Accordingly we obtain N_g^{lb} as

$$(\text{P2}) \quad : \underset{N_g \geq 0}{\text{maximize}}\; N_g \tag{7}$$

$$\text{subject to} \quad \prod_{i=1}^{N_g} \frac{\Phi_1\left(\frac{X_{th}-X_0}{\sigma_i}\right)}{1-\Phi_1\left(-\frac{X_0}{\sigma_i}\right)} \geq 1-\epsilon$$

N_g^{ub} Calculation

- Assuming that X crosses X_{th} in N_gth slot irrespective of whether it had crossed X_{th} before or not, N_g^{ub} is calculated by solving:

$$\text{(P3)} \quad : \underset{N_g \geq 0}{\text{maximize}} \; N_g \tag{8}$$

$$\text{subject to} \quad \frac{\Phi_1\left(\frac{X_{th}-X_0}{\sigma_{N_g}}\right)}{1-\Phi_1\left(\frac{-X_0}{\sigma_{N_g}}\right)} \geq 1-\epsilon$$

- N_g^{lb} and N_g^{ub} allow us to reformulate (5) into an optimization problem with an unimodal objective function

N_g^* Calculation

- Given N_g^{lb} and N_g^{ub}, (5) is reformulated as
  (P4) :

$$N_g^* = \underset{N_g^{lb} \le N_g \le N_g^{ub}}{\operatorname{argmin}} \left[\Pr\left\{X_o + X_1 < X_{th}, \ldots, X_o + X_{N_g} < X_{th}\right\} - (1 - \epsilon \tag{9}$$

- Utilizing unimodal nature of objective function, we propose an algorithm based on Golden Section based line search method[13] to estimate N_g^*

Theorem 1

N_g^* reduces to average fade duration (AFD) with $\epsilon = 0.5$

[13] A. D. Belegundu and T. R. Chandrupatla, *Optimization Concepts and Applications in Engineering*. Cambridge University Press, 2011.

Effect of System Parameters on N_g^*

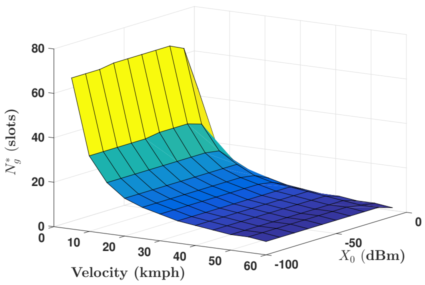

Effect of node velocity and X_0 on N_g^*

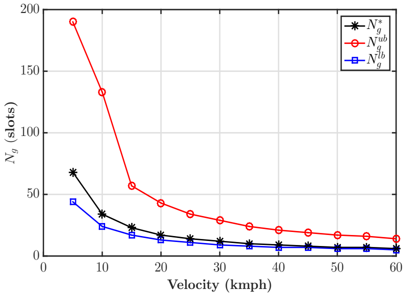

Variation of N_g^{ub}, N_g^*, and N_g^{lb} with velocity

- For same X_0, N_g^* acquires large value for lower node velocity and vice-versa; for $T_p = 500$ μsec, $X_0 = -100$ dBm, $N_g^* = 68$ slots when $v = 5$ kmph compared to $N_g^* = 6$ slots when $v = 60$ kmph
- Lower bound N_g^{lb} is relatively a tighter bound compared to N_g^{ub}

Data Throughput of D-SW

- Duration of ACK/NAK is assumed too small compared to Υ_f, i.e. $\Upsilon_{A/N} = \varrho\Upsilon_f$, where $\varrho \ll 1$
- Channel modeled as a two-state Markov process, $\boldsymbol{M} = \begin{bmatrix} p_{11} & p_{10} \\ p_{01} & p_{00} \end{bmatrix}$
- β-step transition probabilities: $p_{11}(\beta) = \frac{[p_{01}+(1-\delta)^{\beta} p_{10}]}{\delta}$ and $p_{01}(\beta) = \frac{p_{01}[1-(1-\delta)^{\beta}]}{\delta}$, where $\delta = p_{01} + p_{10}$
- If ζ consecutive data transmissions (a R.V) occur thereafter, $\zeta - 1$ are successful, i.e., $\mathbb{E}(\zeta) = \frac{1+p_{10}(\beta)}{p_{10}(\beta)}$
- ***Data throughput*** (D_R): Average number of data frames delivered successfully per second

$$D_R = \frac{A}{B + \frac{CN_g}{1-D^{N_g}}} \quad \text{frames/s} \tag{10}$$

Here $A = \mathbb{E}[\zeta] - 1$, $B = (\mathbb{E}[\zeta] - 1)\beta\Upsilon_f + \Upsilon_f + 3\Upsilon_{A/N}$, $C = \frac{\delta\Upsilon_f}{p_{01}(1)}$, and $D = 1 - \delta$

Energy Consumption of D-SW

- ***Energy consumption per data frame*** (E_B): Energy consumption per successfully delivered data frame
  Let ν_f, $\nu_{A/N}$, ν_i and ν_p denote transmit and receive energy per data frame, transmit and receive energy per ACK/NAK frame, per slot idling energy and per slot total energy consumption per probing frame respectively. Then E_B is

$$E_B = \frac{E + \frac{F}{1-D^{N_g}}(G + N_g H)}{A} \text{Joule} \tag{11}$$

  where $E = \mathbb{E}\left[\zeta\right](\nu_f + \nu_{A/N}) + (\mathbb{E}\left[\zeta\right] - 1)(\beta - 1)\nu_i$, $F = \frac{\delta}{p_{01}(1)}$, $G = \nu_p$, and $H = \nu_i$
- Energy efficiency is defined as $\eta = \frac{\mathcal{D}_{\mathcal{R}}}{\mathcal{E}_{\mathcal{B}}}$
- η needs to higher for a good scheme i.e., a better scheme should provide higher overall efficiency

Optimal ϵ Estimation

- Optimal ϵ estimation for maximizing energy efficiency

$$\text{(P6)} \quad : \underset{\epsilon}{\text{maximize}}\ \eta \tag{12}$$

$$\text{subject to} \quad C1 : 0 \leq \epsilon \leq \epsilon_u, \quad C2 : N_g \geq 1, \quad \text{and}$$

$$C4 : g(X_o, X_{th}, f_D, T_p, \epsilon) = N_g,$$

where function $g(X_o, X_{th}, f_D, T_p, \epsilon)$ gives output N_g^* for a given set of X_o, X_{th}, f_D, and T_p.

$$\epsilon^* = \min\{\epsilon_{opt}, \epsilon_u\}, \text{where} \quad \epsilon_{opt} = \left\{\epsilon_{opt} : g(X_o, X_{th}, f_D, T_p, \epsilon_{opt}) = N_g^*\right\} \tag{13}$$

Competitive Approaches

Prior related approaches: AP1, AP2[14], CT [15]

1. AP1: proposes AFD $\tau(X_{th})$ as the waiting interval T_{bg}
2. AP2: $T_{bg} = 0.5 \times [\tau(X_{th}) - \tau(X_i)]$, where $X_i = X_n + \frac{X_{th}}{2L}$ is the quantized SSI lying in $\{X_n, X_{n+1}\}$ if the entire $\{X \mid X < X_{th}\}$ range is sub-divided into L levels with quantization step size $\frac{X_{th}}{L}$
3. CT: takes coherence time[16] $T_c = \frac{0.423}{f_D}$ as default T_{bg} irrespective of X_0.

- Average Fade duration is mathematically defined as

$$\tau(X_{th}) = \frac{\Pr\{X < X_{th}\}}{\int_0^{\infty} \dot{x} f_{X,\dot{X}}(X_{th}, \dot{x}) d\dot{x}}$$, where $f_{X,\dot{X}}(x, \dot{x})$ is joint PDF of X and $\dot{X}$

[14] S. De, A. Sharma, R. Jantti, and D. H. Cavdar, "Channel adaptive stop-and-wait automatic repeat request protocols for short-range wireless links," *IET Commun.,* vol. 6, no. 14, pp. 2128-2137, Sep. 2012.

[15] H. Moon, "Channel-adaptive Random Access With Discontinuous Channel Measurements," *IEEE J. Sel. Areas Commun.,* vol. 34, no. 5, pp. 1704-1712, May 2016.

[16] T. Rappaport, *Wireless Communications: Principles and Practice*. Prentice Hall PTR, 2001.

Proposed Framework Verification

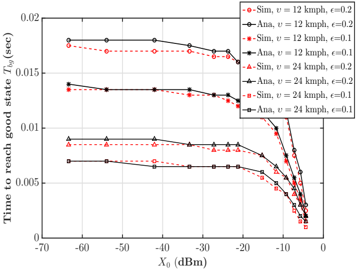

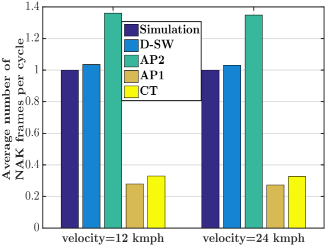

- X_0 plays a key role in T_{bg} estimation
- For a particular X_0, T_{bg} decreases with increasing v; reason being decrease in correlation
- Unlike other approaches, average no. of NAK frames per cycle is close to 1 for D-SW

Energy Efficiency

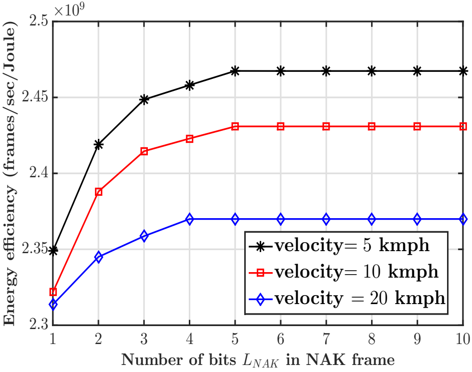

Effect of NAK frame size L_{NAK} on Energy efficiency η

- Initial increase of η with L_{NAK}, leading to η satuaration beyond $L_{NAK} \geq 5$

Performance Comparison

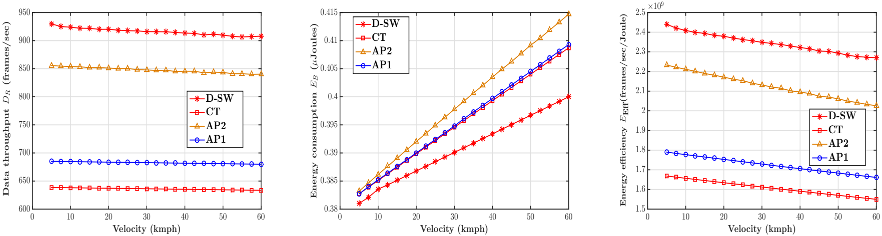

(a) Data rate; (b) Energy consumption; (c)Energy efficiency

- D-SW results in 9% more data throughput, 4% less energy consumption, and 12% more energy-efficient over nearest competitive approach AP2

Remarks

- D-SW estimated the 'waiting time' when channel is not suitable for data transmission, i.e., $X < X_{th}$
- But D-SW fails to exploit channel when it is in 'good' state, i.e., $X \geq X_{th}$
- D-SW only estimates optimal waiting time when channel is unusable for data transmission
- Hence we extend our analysis to the condition when $X \geq X_{th}$

Channel-aware Dynamic Window protocol (cDIP)[17]

- cDIP: a combination of channel-aware SW and SR
- When channel is 'bad' ($X < X_{th}$), cDIP waits for time $\boldsymbol{T_{bg}} = N_g^* \cdot T_p$ until channel becomes usable
- When channel is 'good' ($X \geq X_{th}$), as in SR, Tx continuously transmits data frames for time $\boldsymbol{T_{gb}} = N_b^* \cdot T_p$ without waiting for an ACK/NAK
- Unlike classical SR, only NAK packets are sent for incorrectly received data packets, which are retransmitted by the Tx

[17] P. Mukherjee and S. De, "cDIP: Channel-aware dynamic window protocol for Energy-efficient IoT Communication ," *IEEE Internet Things J.*, vol. 5, no. 6, pp. 4474-4485, Dec 2018.

cDIP Algorithm

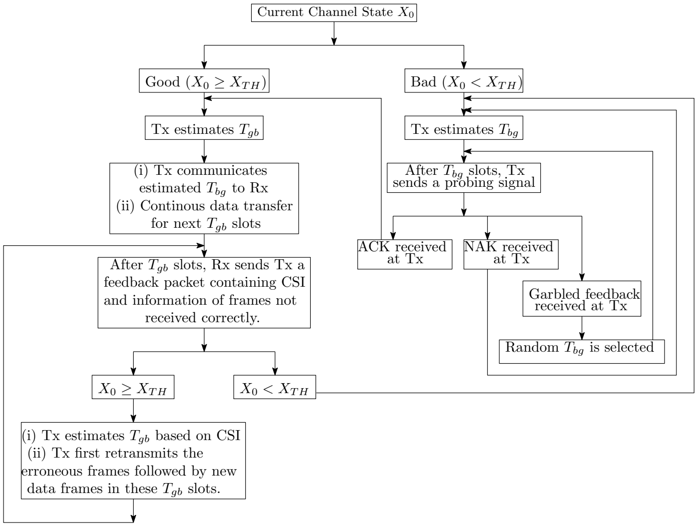

T_{gb} estimation

- $\boldsymbol{T_{gb}} = N_b^* \cdot T_p$, where N_b^* is the estimated time interval that $X \geq X_{th}$ when $X_0 \geq X_{th}$
- N_b^* is calculated by solving:

$$(\text{P7}) \quad : \underset{N_b \geq 0}{\text{maximize}}\ N_b \tag{14}$$

subject to

$$\Pr\left\{X_0 + X_1 \geq X_{th}, \cdots, X_0 + X_{N_b} \geq X_{th}\right\} \geq 1 - \epsilon$$

- Here also $X_1, \cdots, X_{N_b}$ are truncated Gaussian R.Vs as stated earlier
- P7 is reformulated like P1 to obtain N_b^*

TO SUMMARIZE:

- P1 estimated time N_g^* for which Tx can be put to sleep when the channel is unusable.
- P7 estimated time N_b^* for which Tx can continuously transmit data without waiting for any ACK/NAK when the channel is suitable for communication

Data throughput of cDIP

- Data throughput: Long-term average of successfully delivered data frames per second.

$$D_T = \frac{\frac{(1-\epsilon)}{\zeta}\overline{N_b}}{(\overline{N_b} + \overline{N_g})T_p + 3T_{fp}} \quad \text{frames/sec} \tag{15}$$

  - ζ : interval between two consecutive data frame transmission attempts
  - $\overline{N_b}$ and $\overline{N_g}$: long-term averages of N_b^* and N_g^* respectively, i.e.,

    $\overline{N_b} = \lim_{N\to\infty} \frac{1}{N} \sum_{i=1}^{N} N_b^*(i)$ and $\overline{N_g} = \lim_{N\to\infty} \frac{1}{N} \sum_{i=1}^{N} N_g^*(i)$
  - $3T_{fp}$: time period due to probing based three way handshake between Rx and Tx

Energy consumption of cDIP

- Energy consumption: Long-term average energy consumption per successfully delivered data frame.

$$E_C = \frac{\frac{\overline{N_b^*}}{\zeta}\nu_f + 2\nu_{A/N} + \nu_p + (\overline{N_b^*} + \overline{\alpha_{bg}})\nu_i}{\frac{(1-\epsilon)}{\zeta}\overline{N_b^*}} \quad \text{Joules} \tag{16}$$

$\nu_f, \nu_{A/N}, \nu_p$, and ν_i : transmit and receive energy per data frame, transmit and receive energy per ACK/NAK frame, probing frame, and per slot idling energy

- Energy efficiency: $\eta = \frac{D_T}{E_C}$ frames/sec/Joule
- User-defined range of ϵ: $\epsilon \in [\epsilon_l, \epsilon_u]$
- Optimization problem P8 formulated to obtain ϵ^* (optimal ϵ):

$$(\text{P8}) : \epsilon^* = \left\{ \epsilon \,\middle|\, \underset{\epsilon_l \leq \epsilon \leq \epsilon_u}{\text{argmax}}\, \eta \right\} \tag{17}$$

Verification of T_{gb} estimation

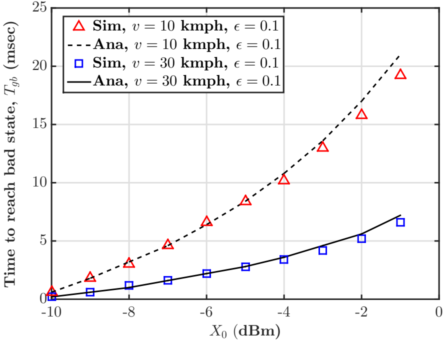

Verification of T_{gb} estimation via Monte Carlo simulation. $X_{TH} = -10.4576$ dBm

- $X_0 \gg X_{TH}$ is not the same as X_0 being just more than X_{TH}
- Rate of increase of T_{gb} with X_0 increases with decreasing v

Effect of Fading Margin

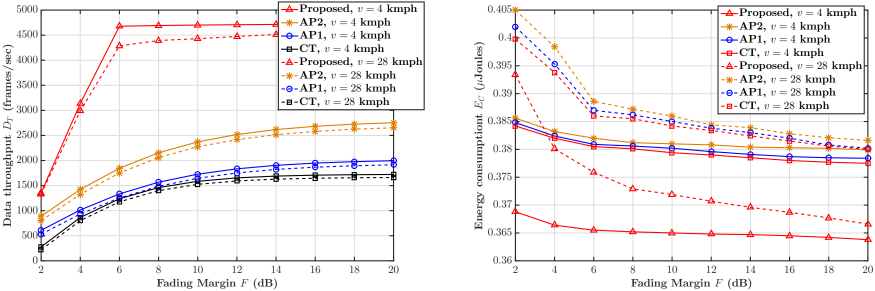

Effect of fading margin F on performance of cDIP

- Increasing F implies that channel is more likely to stay in 'good' state most of the time
- cDIP unlike AP1, AP2, or CT avoids regular feedbacks even when channel is in 'good' state
- This results in significant performance improvement

Overhead Performance

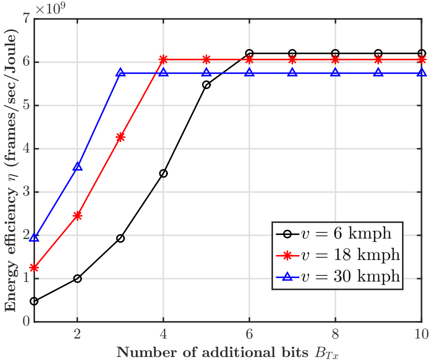

Effect of overhead B_{Tx} on η of cDIP. $\epsilon = 0.05$, and $X_{TH} = -3.9788$ dBm

- B_{Tx} in case of cDIP, just like L_{NAK} of D-SW, initially leads to energy-efficiency enhancement before saturating at some point
- Lower node mobility requires higher $B_{Tx}^{\text{satuarate}}$, which reaffirms our observation made in the analysis-simulation plot

Performance Comparison

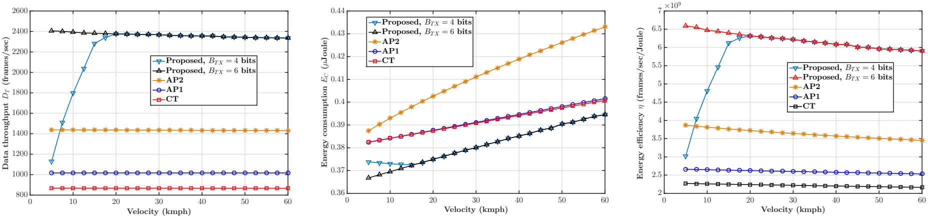

Performance comparison: (a) Data throughput; (b) Energy consumption; (c) Energy efficiency. $X_{TH} = -3.9788$ dBm

- Approximately 40.18% higher throughput, 9% lower energy consumption, and 41.92% higher energy efficiency with respect to AP2
- Nominal extra overhead
- Gain margin increases considerably compared to D-SW

Summary on Cross-layer Adaptive Protocols

- Presented the research case studies on cross-layer channel aware link-layer protocols
- Significant energy efficiency can be achieved through simple extension of PHY-layer information exchange
- Further significant improvement of energy efficiency is achievable through more fundamental information exchange
- The proposed techniques are general, i.e., *they are agnostic to the channel envelop distribution*

II: Data-driven Smart IoT Framework[18]

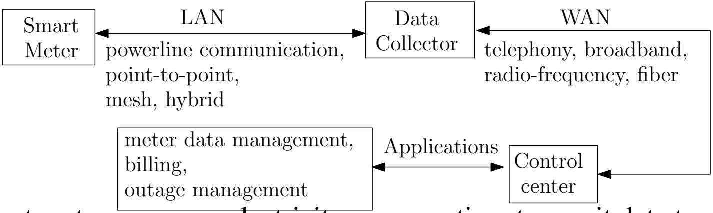

- Smart meter: measure electricity consumption, transmit data to collector
- Sampling Rate: From 1 sample/sec to 1 sample per several minutes
- Data collector: retrieves the data, may or may not process the data
- Control center: central data collection point, data processing

Motivation and Research Gap:

- High resolution smart meter data essential for near real-time applications
- Characterization of high resolution smart meter data difficult due to spiky and fluctuating load patterns

[18] S. Tripathi and S. De, "An efficient data characterization and reduction scheme for smart metering infrastructure", *IEEE Trans. Ind. Informat.*, vol. 14, no. 10, 2018.

Characterization of Smart Meter data

- Dataset used:
  1. Reference Energy Disaggregation Dataset (REDD) published by Massachusetts Institute of Technology (MIT) sampled at 1 sample/sec[19]
  2. Locally available real smart meter data sampled at 1 sample/ 30 seconds

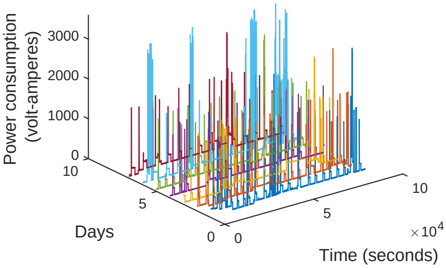

Daily consumption of a household for 7 days

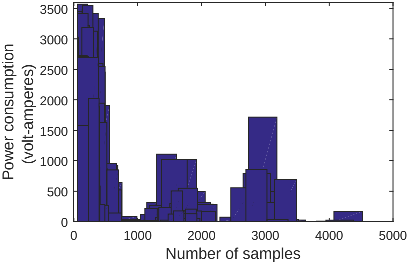

Histogram of power consumption

- From the histogram plot GM model for smart meter data characterization

[19] J. Kolter and M.Johnson, "Redd: A public dataset for energy disaggregation and research", in *Proc.Workshop Data Min. Appl. Sustain.*, San Diego, CA, USA, 2011, pp. 1–6.

Model Parameter Selection

- For load profile having N data points $\{x = x_1, x_2, \ldots, x_N\}$, GMM consisting of k-components expressed as:

$$f_k(x) = \sum_{j=1}^{k} w_j \mathcal{N}(x|\mu_j, \sigma_j), \text{with} \quad w_j \geq 0 \quad \text{and} \quad \sum_{j=1}^{k} w_j = 1$$

- For different k, optimal μ_j, σ_j, w_j determined by maximizing log-likelihood function using Expectation-Maximization (EM) algorithm
- Hellinger's distance[20] metric used as measure of goodness of fit
- For discrete probability distributions $P = \{p_1, p_2, \cdots, p_n\}$ and $Q = \{q_1, q_2, \cdots, q_n\}$, Hellinger's distance between them is defined as:

$$H(P, Q) = \frac{1}{\sqrt{2}} \sqrt{\sum_{i=1}^{n} (\sqrt{p_i} - \sqrt{q_i})^2}$$

[20] A. L. Gibbs and F. E. Su, "On choosing and bounding probability metrics", *Intl. Statistical Rev.*, vol. 70, no. 3, pp. 419–435, 2002.

Model Fitness

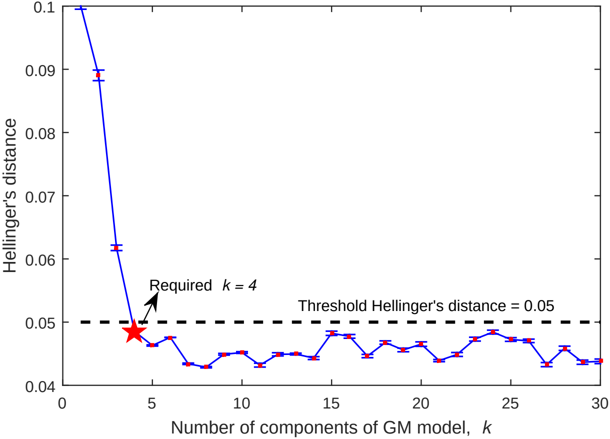

- Acceptable threshold of Hellinger's distance between two pdfs is 0.05[21]
- Beyond $k = 4$, Hellinger's distance falls below threshold
- Computation complexity of k-GM model increases as $\mathcal{O}(kn^2)$

[21] L. Pardo, *Statistical Inference Based on Divergence Measures*. CRC Press, 2005.

GMM Parameters

- GMM parameters for $k = 4$ are estimated using EM algorithm and shown in Table:

k	1	2	3	4
μ_j (VA)	58.053	131.50	291.20	1783.6
σ_j (VA)	5.2967	106.2834	8.001×10^3	1.221×10^5
w_j	0.098	0.529	0.34	0.033

Comparison with Existing Characterization models

- CDF of 4- component Gaussian mixtures compared with the existing data characterization models against the empirical CDF in Fig. ??.

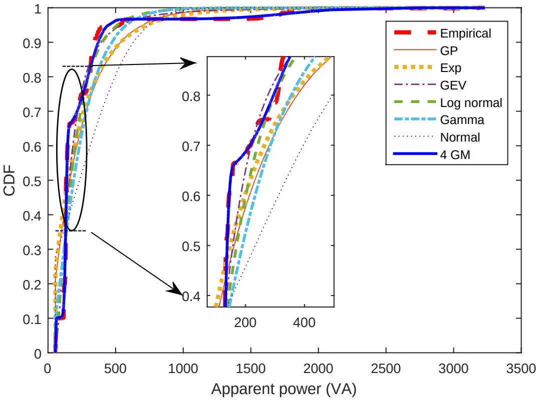

Model Fitness Comparison

Distribution fits	Hellinger's distance
Normal	0.0872
Exponential	0.0866
Generalized Pareto (GP)	0.0866
Gamma	0.0832
Log normal	0.0803
Generalized extreme value (GEV)	0.0784
2 GM model	0.0725
3 GM model	0.0446
4 GM model	0.0379
5 GM model	0.0373
6 GM model	0.0370

- Hellinger's distance above acceptable threshold for existing characterization models
- Hellinger's distance fairly constant up to 3 decimal places for GM models with $k \geq 4$
- *Thus, daily power consumption data sampled at 1 Hz frequency by the smart meter is reasonably characterized using 4-component GM model*

Compressive Sampling

- Compressive sampling (CS) scheme for data reduction to compress high frequency smart meter data without any loss of information
- In CS[22], measured value of load profile x is denoted by y:

$$y = \Phi.x \tag{18}$$

Φ: sensing matrix of size $N \times N$, N: number of samples in data collection window, and y, x: vectors of size $N \times 1$

- Further, decomposing x using a sparse basis φ of size $N \times N$,

$$x = \varphi.f \tag{19}$$

f is a column vector of coefficients corresponding to φ of size $N \times 1$

- Only m ($m \ll N$) samples are chosen for transmission, then

$$\hat{y} = \hat{\Phi}.\varphi.f = \hat{A}.f \quad \text{or} \quad \hat{A} = \hat{\Phi}.\varphi \tag{20}$$

$\hat{y}$ is $m \times 1$ vector, f is $N \times 1$ vector, $\hat{A}$ and $\hat{\Phi}$ are $m \times N$ matrices

[22] E. J. Candes and M. B. Wakin, "An introduction to compressive sampling", *IEEE Signal Process. Mag.*, vol. 25, pp. 21–30, 2008.

Conditions for Accurate Reconstruction

- Accurate reconstruction of Fourier/DCT coefficients f from undersampled system is challenging due to need of solving an underdetermined linear system of equations
- Compressive sampling enables exact reconstruction of f from $\hat{y}$, if the signal is s-sparse in some basis using l_1 minimization formulation[23]
- Sensing matrix Φ and basis matrix φ should be incoherent for smaller value of m/N[24]
- Restricted Isometry Property (RIP)[25] should be satisfied between sensing matrix Φ and basis matrix φ for lower reconstruction error

[23] E. Candes, J. Romberg, and T. Tao, "Robust uncertainty principles exact signal reconstruction from highly incomplete frequency information", *IEEE Trans. Inf. Theory*, vol. 52, pp. 489–509, 2006.

[24] E. J. Candes and Romberg, "Sparsity and incoherence in compressive sampling", *Inverse Problems*, vol. 23, no. 3, pp. 969–985, 2007.

[25] E. J. Candes and T. Tao, "Decoding by linear programming", *IEEE Trans. Inf. Theory*, vol. 51, no. 12, pp. 4203–4215, 2005.

Proposed Adaptive Compressive Sampling Algorithm

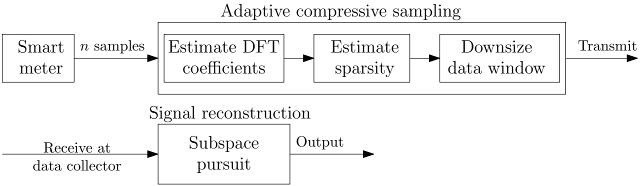

- Choice of Parameters:
  - Sensing matrix Φ: Random normal matrix with mean $1/m$ and variance of size (m,N)

    N = number of samples in the data window

    m = number of samples transmitted to data collector
  - Sparse basis matrix φ: Discrete Fourier transform
- Sparsity NOT assumed to be known apriori
- Sparsity decided for every data window by estimating the number of DFT coefficients containing 99.99% energy
- Number of samples to be transmitted m out of N, $m = s \log(\mathrm{N})$[26]

[26] A. Unterweger and D. Engel, "Resumable load data compression in smart grids", *IEEE Trans. Smart Grid*, vol. 6, no. 2, pp. 919–929, 2015.

Optimum Data Collection Interval Estimation

- Bandwidth saving: $\frac{(N-m)}{N}$
- $\Uparrow$ data collection window size N
  $\Rightarrow$
  $\Downarrow$ RMSE , $\Downarrow$ Bandwidth saving
- Trade off between data reconstruction accuracy and bandwidth requirement
- RMSE saturates beyond $N = 600$ samples, while bandwidth saving keeps deteriorating
- Optimum data collection interval $N_{opt} = 600$ samples or 10 mins; bandwidth saving: 39.9%

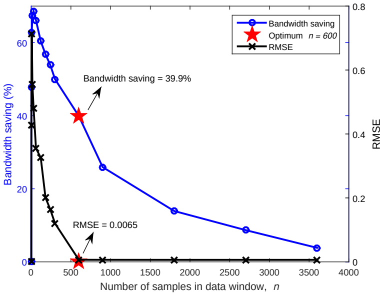

- *Thus, by applying adaptive compressed sampling technique and updating data at the collector every 10 minutes, about 40% reduction in bandwidth requirement can be achieved.*

Reconstruction Performance of Compressed Sampling

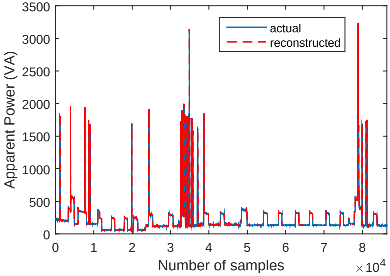

Reconstructed data for 10 minutes interval versus actual data for house 1

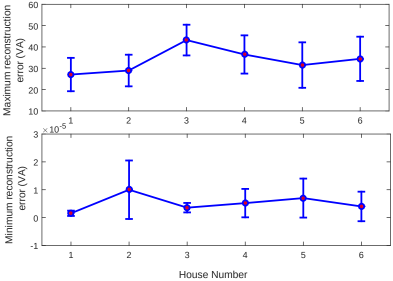

Maximum and minimum reconstruction error for all houses

- Reconstructed data closely follows actual data, RMSE in first Fig. = 0.0065
- Data windows with more spikes ⇒ maximum difference between actual samples and reconstructed samples could be large

Characterization of Reconstructed Data using 4-GM model

- Hellinger's distance between empirical and reconstructed smart meter data = 0.0398
- Parameter estimates of 4-GM model for the reconstructed smart meter data in Table below

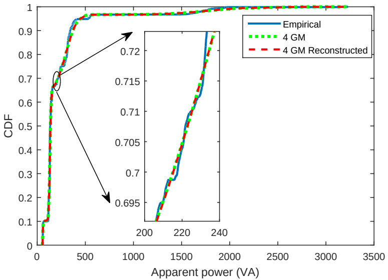

Comparison of CDFs of empirical versus 4-GM modeled and 4-GM reconstructed over 10 mins

4-GM model parameter estimates for reconstructed smart meter data

k	1	2	3	4
$\hat{\mu}_j$ (VA)	58	131.9	297.3	1782.9
$\hat{\sigma}_j$ (VA)	5.5633	106.4793	8.081×10^3	1.221×10^5
$\hat{w}_j$	0.0991	0.5421	0.3257	0.0331

- GM parameters in modeled original data versus that after reconstruction: $\Rightarrow$ structural features of data before compression are restored after data reconstruction at data collector
- *Thus, bandwidth saving is achieved with minimal information loss in data compression process*

Compression Performance Comparison with[27]

Sampling rate: 1 sample/sec

- Resumable load data compression (RLDC) [Candes and Tao, "Decoding by linear programming," IEEE Trans. Inf. Theory, vol. 51, no. 12, 2005] is lossless
- Adaptive compressive sampling: $\Uparrow$ interval size, bandwidth saving $\Downarrow$
- At N_{opt}= 10 minutes, improvement in bandwidth saving over RLDC = 23.7%

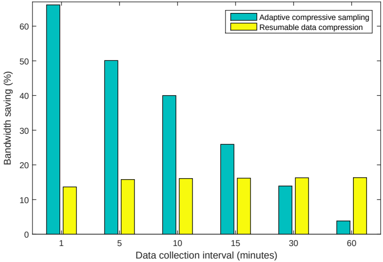

Adaptive compressive sampling vs RLDC at different data collection intervals, 1 sample/sec.

[27] W. Dai and O. Milenkovic, "Subspace pursuit for compressive sensing: Closing the gap between performance and complexity", *IEEE Trans. Inf. Theory*, vol. 55, no. 5, pp. 2230–2249, 2009.

Effect of Increasing Sampling Interval

Dataset	Adaptive compressive sampling		Resumable data compression
	RMSE	Bandwidth saving	Bandwidth saving
1	0.0277	22.63%	-3.35%
2	0.0574	5.75%	-5.35%
3	0.0598	27.79%	0.8%
4	0.0683	16.58%	-4.17%
5	0.0611	16.88%	-9.8%
6	0.0437	27.58%	4.92%

- Sampling rate: 1 sample/30 sec
  - Lesser correlation ⇒ larger consecutive value difference
  - As compared to 1 second, mean reduction in bandwidth savings: 20.37% and 33.26%, respectively, for adaptive compressive sampling and RLDC.
  - With 30 second sampling interval, improvement in bandwidth saving over RLDC = 22.4% at the cost of increased RMSE
- *Thus, adaptive compressive sampling technique outperforms RLDC in bandwidth saving both at 1 second and 30 seconds sampling interval.*

Effect of Channel Noise

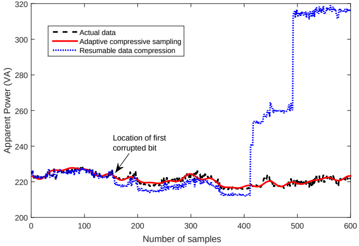

Reconstruction with 1% corrupted samples in adaptive compressive sampling and RLDC

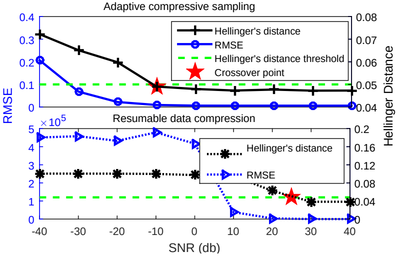

Variation of RMSE with SNR in adaptive compressive sampling and RLDC

- With 1% corrupted samples in a transmission window: Adaptive compressive sampling $\Rightarrow$ data is recoverable
- Adaptive compressive sampling $\Rightarrow$ acceptable for at SNR, $\sim\ -10$ dB RLDC $\Rightarrow$ acceptable for SNR $= 30$ dB and above
- *Thus, adaptive compressive sampling technique is more robust*

Modified Smart Metering Architecture

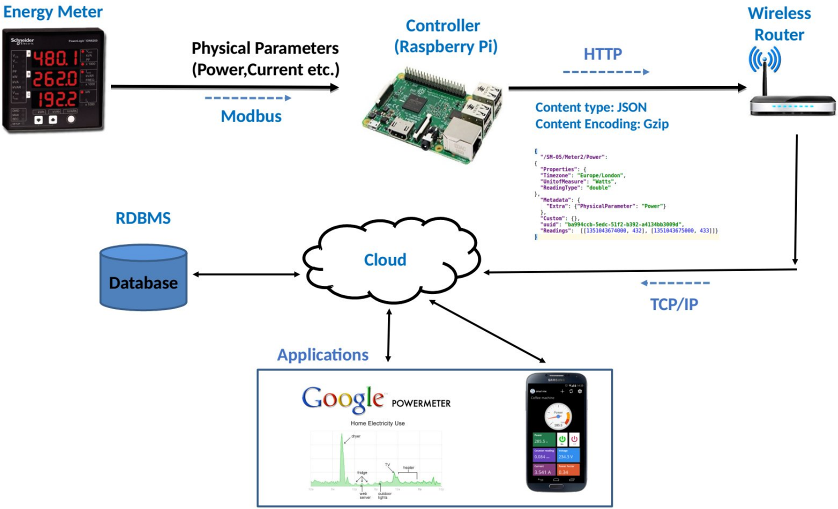

Implementation on Real Systems

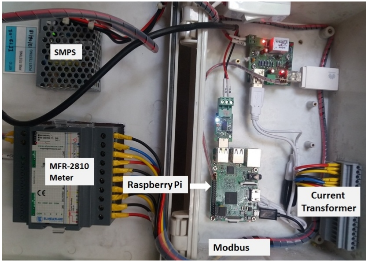

Figure 1: Smart meters installed at IITD

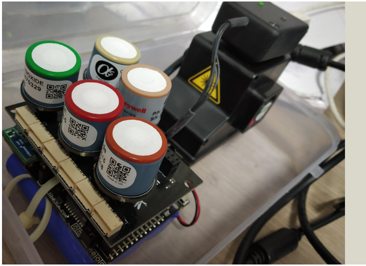

Figure 2: Air quality monitoring

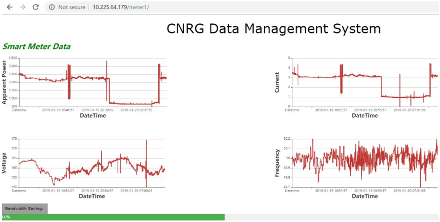

Figure 3: Web interface of cloud storage

Summary:

- Energy, storage and bandwidth efficiency
- Node-computing in capable devices
- Edge-computing for res. constrained nodes

Summary on Data-driven Smart IoT

- High frequency smart meter data characterized using gaussian mixture model with 4 components, which is used in evaluating the quality of data reduction at the smart meter.
- Compressive sampling based scheme devised for adaptive data reduction at the smart meter
- Optimum data collection interval estimated empirically to be 10 minutes
- While collecting and processing smart meter data at 10 minutes interval, around 40% reduction in bandwidth requirement is achieved at individual smart meter level
- Compared to existing competitive approach in [20], adaptive compressive sampling scheme demonstrates robustness in reconstruction with acceptable accuracy and around 23.4% and 22.4% more bandwidth saving on smart meter data sampled respectively at 1 second and 30 seconds intervals

Networked Sensing

- **Requirement:** durable/sustainable **W**ireless **S**ensor **N**etworks
- **Limitation:** Battery constrained sensor nodes (SNs)
- **Solution:** Intelligent sensing (sense using a few SNs, estimate entire field)
- **Sensor selection strategies:**
  * Centralized scheme[28],[29]: Sensing decision taken at fusion center
  * Decentralized scheme[30]: Sensing decision taken at node level
  * Multi-sensing of parameters in heterogeneous WSNs

Idea

Efficient sensor selection = *f(process dynamics, sensing quality, dynamic energy resource of SN)*

- **Applications:** Smart environment, smart agriculture, pollution monitoring, source localization, battlefield surveillance, landslides detection

[28] W. Chen and I. J. Wassell, "Optimized node selection for compressive sleeping wireless sensor networks", *IEEE Trans. Veh. Technol.*, 2016.

[29] G. Quer, R. Masiero, G. Pillonetto, M. Rossi, and M. Zorzi, "Sensing, compression, and recovery for WSNs: Sparse signal modeling and monitoring framework", *IEEE Trans. Wireless Commun.*, 2016.

[30] S. Hwang, R. Ran, J. Yang, and D. K. Kim, "Multivariated bayesian compressive sensing in wireless sensor networks", *IEEE Trans. Sensors J.*, 2015.

Centralized Sensor Selection

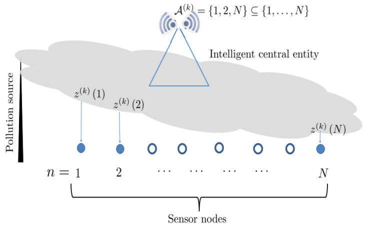

Densely deployed WSN

Research Gap

-Constant sparsity assumption for a process
-Energy-inefficient adaptation
-Same resource cost of SNs

-System model during k^{th} measurement cycle,

$$\tilde{\mathbf{y}}^{(k)} = \mathbf{A}^{(k)}\mathbf{z}^{(k)} + \mathbf{n}^{(k)}. \qquad (21)$$

Proposed Centralized Framework[10]

-**Multi-objective optimization:** trade-off b/w sensing quality and energy efficiency

-Verified framework on synthetic and real data sets of WSN

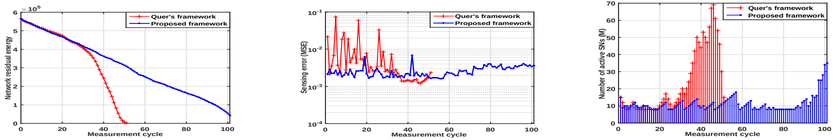

(a) N/w residual energy **(b)** Sensing quality **(c)** No. of active SNs

Figure 4: Comparison of the proposed framework with the Quer's framework[31].

[31] V. Gupta and S. De, "SbI-based adaptive sensing framework for WSN-assisted IoT applications", *IEEE IoT J.*, 2018.

Decentralized Sensor Selection

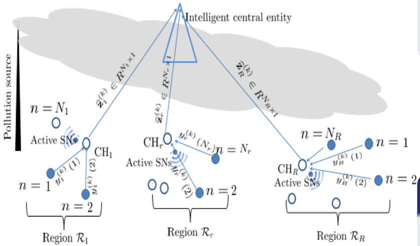

Decentralized WSN system

Research Gap

-Energy consumption not accounted
-Non-adaptive to process dynamics

-Regional system model during k^{th} cycle,

$$\mathbf{y}_r^{(k)} = \mathbf{A}_r^{(k)}\mathbf{z}_r^{(k)} + \mathbf{n}_r^{(k)}, \ 1 \leq r \leq R. \quad (22)$$

Proposed Decentralized Framework[11]

-Quality-efficiency trade-off
-Accounts energy consumption in each step
-Retraining logic (limit error accumulation)

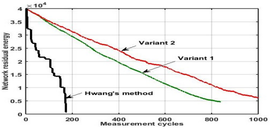

(a) N/w lifetime

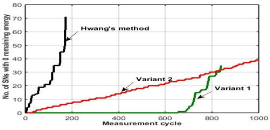

(b) Node lifetime

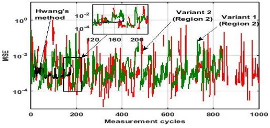

(c) Sensing quality

Comparison of the proposed framework with Hwang's approach

Multi-Sensing

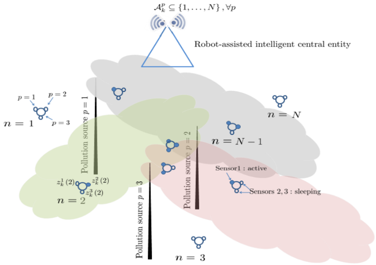

EH-WSN (N nodes, P sensors, slow proc.)

Research Gap

- -Dedicated nodes for sensing each parameter
- -Hierarchical models for dependent parameters
- -No focus on sensor selection & estimation

-System model during k^{th} measurement cycle,

$$\tilde{\mathbf{y}}_k^p = \mathbf{A}_k^p \mathbf{z}_k^p + \mathbf{n}_k^p, \ \forall 1 \leq p \leq P. \qquad (23)$$

Proposed Multi-sensing Framework[12]

- -Sensing quality - energy efficiency tradeoff
- -Predicts active sensors for next cycle

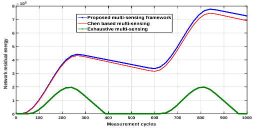

(d) Energy efficiency

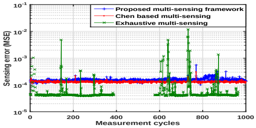

(e) SO_2 sensing error

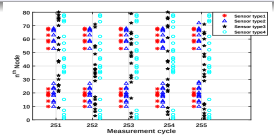

(f) Active sensors pattern

Comparison of the proposed framework with Chen's[32] and exhaustive multi-sensing

[32] V. Gupta and S. De, "Adaptive multi-sensing in EH-WSN for smart environment", 2019.

Summary on Cross-layer Optimization

- Presented the case studies on channel aware link-layer protocols
- Significant energy efficiency can be achieved through simple extension of PHY-layer information exchange
- Further significant improvement of energy efficiency is achievable through more fundamental information exchange
- The proposed techniques are general, i.e., *they are agnostic to the channel envelop distribution*
- In typical IoT networks, non-stationarity of data is frequently encountered
- In general, stochastic models fail to adapt to the changing dynamics of the real world processes
- Data-driven approaches capable of continuous updation of underlying model address this issue
- With evolving edge analytics, availability of sufficient hardware configurations facilitates implementation of data-driven algorithms

Queries

IITD-CNRG Website:
http://cnrg.iitd.ac.in/
Contact: swadesd@ee.iitd.ac.in

Thanks!